2016

Separation of Liquid and Vapor in Header of MCHE

Jun Li
ACRC, University of Illinois at Urbana-Champaign, United States of America, junli9@illinois.edu

Pega Hrnjak
pega@illinois.edu

Separation of Liquid and Vapor in Header of MCHE

Jun LI[1], Pega HRNJAK[1,2]*

[1]Department of Mechanical Science and Engineering,
University of Illinois at Urbana-Champaign
Urbana, IL, USA
junli9@illinois.edu

[2]Creative Thermal Solution
Urbana, IL, USA
pega@illinois.edu

* Corresponding Author

ABSTRACT

This paper presents the experimental study of separation of two-phase flow in a vertical header of microchannel heat exchanger (MCHE) based on quantified visualization using fast camera, modelling analysis and experimental evaluation. A condenser model is developed to explore separation effects on heat exchanger. The modeling results show the benefits that a separation condenser has over a conventional condenser is affected by the separation results in the header. A header prototype is made that has an inlet in the longitudinal center part. Two sub-passes downstream are incorporated, lower for liquid and upper vapor flow. The header for experiment is clear to provide visual access. R-134a is used as the fluid of interest and mass flux through the inlet microchannels is controlled between 55 kg/(m^{2}s)-195 kg/(m^{2}s). The experiment results indicate that ideal separation in that header can happen at low mass flux up to 70 kg/(m^{2}s). Results are presented in function of liquid and vapor separation efficiencies (η_l, η_v). Two phase flow inside the header is analyzed to study the mechanisms for liquid-vapor separation.

1. INTRODUCTION

MCHEs are widely used in Heating, Ventilation, Air-Conditioning & Refrigeration (HVAC&R) industry due to their high overall heat transfer coefficient, lower refrigerant inventory, compactness and lower weight. Air side was known for having the major heat resistance in heat transfer for a MCHE. However, with fin design being innovated and revolutionized, the resultant larger air-side area and heat transfer gives a promising prospect of enhancing the refrigerant-side heat transfer coefficient or contact area. For a heat transfer process, liquid on the wall of condenser is detrimental while vapor on the wall of evaporator detrimental. Removing unwanted phase is one of the options to improve heat transfer and reduce pressure drop.

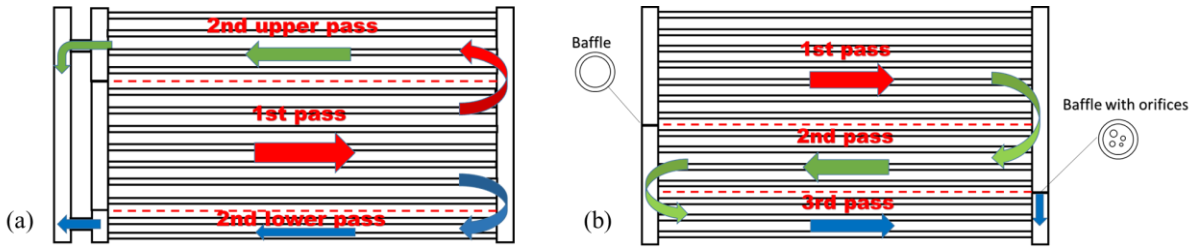

Figure 1: Methodologies to remove unwanted phase in MCHE: (a) Separation; (b) Drainage

For a condenser, removing unwanted phase may refer to separating liquid from vapor in an intermediate header and then sending liquid to a small volume of the following flow passage [Figure 1(a)]. Or draining the generated liquid out of the condenser or sending to further downstream pass during condensation process [Figure 1(b)]. Either separation or drainage may be realized via flow passage arrangement / smart circuiting without too much additional

cost. While drainage condensers have been extensively studied by Wu *et al.* (2003) and Zhong *et al.* (2014), quantitative study on separation inside the header is rarely found in open literature. The idea of separation condenser was first proposed by Oh *et al.* (2003), named as a multistage gas and liquid phase separation condenser. The schematic is shown in Figure 2. It has a combining receiver for the upper vapor pass and lower liquid pass and a designated sub-cooling pass. The authors claimed that the invention can enhance the subcooling in the 2nd-liquid pass as well as in the subcooling pass.

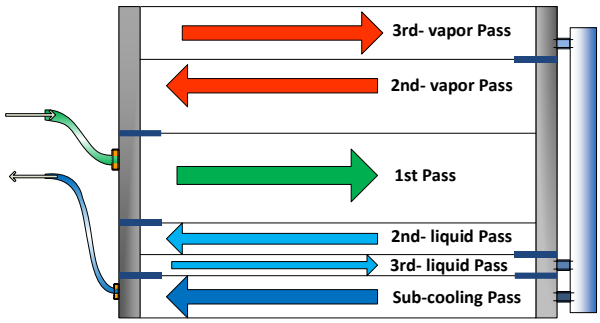

Figure 2: A schematic design of microchannel condenser with separation, Oh *et al.* (2003)

The theoretical rationale behind the advantages of a separation condenser is following. For a condensation process at the same mass flux, the high-quality (0.8-1) two-phase refrigerant has 10-15 times higher heat transfer coefficient than a low-quality (0.1-0.3) two-phase refrigerant, depending on the category of refrigerant. When condenser face area and total heat transfer area are fixed, smart circuiting can potentially improve heat transfer performance by utilizing the high heat transfer coefficient of separated vapor and giving more heat transfer area (more microchannel tubes) to this vapor flow. If the mass flux of vapor can be kept the same with non-separated refrigerant, it should have a much higher heat transfer coefficient. Overall, it will enhance the heat transfer of the condenser.

Because of the complexity of two-phase flow in header structures, it is almost inevitable to feed non-homogeneous refrigerant flow into each microchannel tube in a MCHE. While this kind of non-uniform distribution (maldistribution) of two-phase flow into microchannel tubes exists as a problem, it provides an opportunity to use vapor-liquid separation. Maldistribution has been observed and extensively studied by many scholars (Tuo and Hrnjak, 2013; Zou and Hrnjak, 2013; Li and Hrnjak, 2014). On the other hand, Ye *et al.* (2009) observed a clear and stable vapor-liquid interface in an intermediate header of a multi-pass microchannel condenser, but a quantification of the phase separation has yet to be seen. Oil and vapor refrigerant separation has been investigated by Xu and Hrnjak (2016). Meanwhile, two-phase distribution can also be improved by first separating the liquid and vapor because each phase after separation has more uniform properties than a two-phase flow.

A valid question would then be how much separation really exists in the second header of a MCHE, as shown in Figure 2, and how much is the effect of separation on a condenser performance and further on an air-conditioning system. The scientific merit of this paper is to quantify the effect of liquid-vapor phase separation on the performance of a condenser. Also, this research provides both a quantitative and visual understanding of two-phase refrigerant separation in intermediate headers and studies the corresponding separation mechanisms.

2. COMPARISON OF SEPARATION CONDENSER WITH BASELINE CONDENSER

2.1 Model Description

To verify that phase separation will improve performance for HEs, an empirical model for microchannel condensers has been built up for simulation. Finite volume method is used as the discretization scheme. Following assumptions are made to simplify the model: (1) Refrigerant distribution is uniform among microchannel tubes in each pass; (2) no heat is conducted along the tube or between tube and fins; (3) all headers are adiabatic; (4) incoming air has uniform temperature and velocity profile.

Classic correlations are adopted in the model. Air-side heat transfer and pressure drop correlations are from Chang and Wang (1997) and Chang and Wang (1996), respectively. Heat transfer correlation for single-phase refrigerant is

from Gnielinski (1976) and pressure drop from Churchill (1977). Two-phase region heat transfer and frictional pressure drop correlation is from Cavallini *et al.* (2006) and deceleration pressure drop from Cavallini *et al.* (2009).

Two types of microchannel condensers shown in Figure 3 have been compared via modeling: Figure 3(a) is a 3-pass traditional baseline; Figure 3(b) is a 3-pass condenser with separation circuiting (separation condenser). Both condensers are parallel-flow, single-slab condensers with louver fins. Tube numbers are shown for each pass. The other geometries for the two condensers are kept the same such as length, height, fin geometries, microchannels, etc. Table 1 presents the main geometry for simulated condensers.

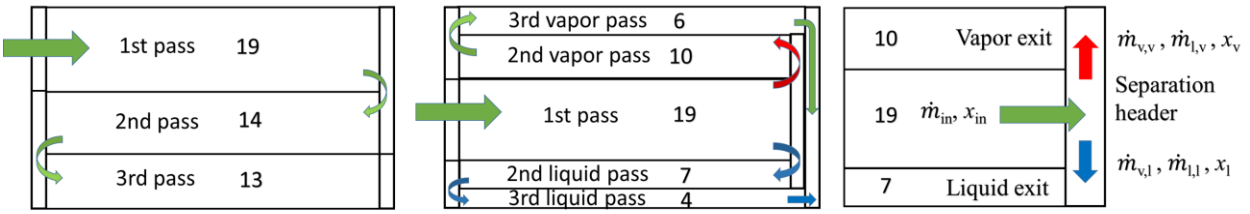

(a) (b) (c)

Figure 3: Condensers for comparison: (a) Baseline condenser; (b) Separation condenser; (c) Zoom in of the separation header

Table 1: Main geometries of the simulated microchannel condensers

Item	**Number**
Tube length	680 mm
Tube pitch	6.8 mm
Total tube number	46
Flow depth	13.6 mm
Fin height	5.8 mm
Fin pitch	1.29 mm
Louver length	4 mm
Microchannel port D_h	0.65 mm
Microchannel ports	17

Figure 3(c) shows the nomenclature of the separation header, which is the second header from Figure 3(b). x_v and x_l denote the quality at the vapor exit and the quality at the liquid exit, respectively. They are calculated as

$$x_v = \frac{\dot{m}_{v,v}}{\dot{m}_{v,v} + \dot{m}_{l,v}} \tag{1}$$

$$x_l = \frac{\dot{m}_{v,l}}{\dot{m}_{v,l} + \dot{m}_{l,l}} \tag{2}$$

where $\dot{m}_{v,v}$ and $\dot{m}_{l,v}$ are the vapor mass flow rate and liquid mass flow rate, respectively, at the vapor exit; $\dot{m}_{v,l}$ and $\dot{m}_{l,l}$ are the vapor mass flow rate and liquid mass flow rate, respectively, at the liquid exit.

x_v is first assumed for every simulation case with a certain inlet condition ($\dot{m}_{in}$, x_{in}) for the header. Different x_v represents different separation result in the header. When $x_v > x_{in}$, phase separation happens. Then, mass flow rate coming into the vapor pass $\dot{m}_v$ is iterated for assumed x_v to balance the pressure drop along the vapor pass and liquid pass.

2.2 Comparison of the two condensers

The first comparison criteria is to compare the refrigerant outlet temperature T_{cdro} for baseline and separation condensers while refrigerant inlet temperature T_{cdri}, refrigerant inlet pressure P_{cdri}, mass flow rate $\dot{m}$, and air conditions are kept the same. T_{cdri} is varying on an isentropic line for each simulation case. The inlet

entropy and refrigerant mass flow rate are decided by experiment data for a real separation condenser.

Comparison is done for two air conditions per SAE Standard J2765 (2008) and results are in Figure 4. It is evident that separation condenser has a lower T_{cdro} than the baseline, which means it has a better heat transfer performance. The biggest difference is 1.1°C for simulated conditions. $\dot{m}_{in}$ and x_{in} are marked for each graph. With $x_v > x_{in}$, separation happens for these assumed x_v. In addition, the difference on T_{cdro} changes with x_v. Therefore, separation in the header has an impact on heat transfer performance.

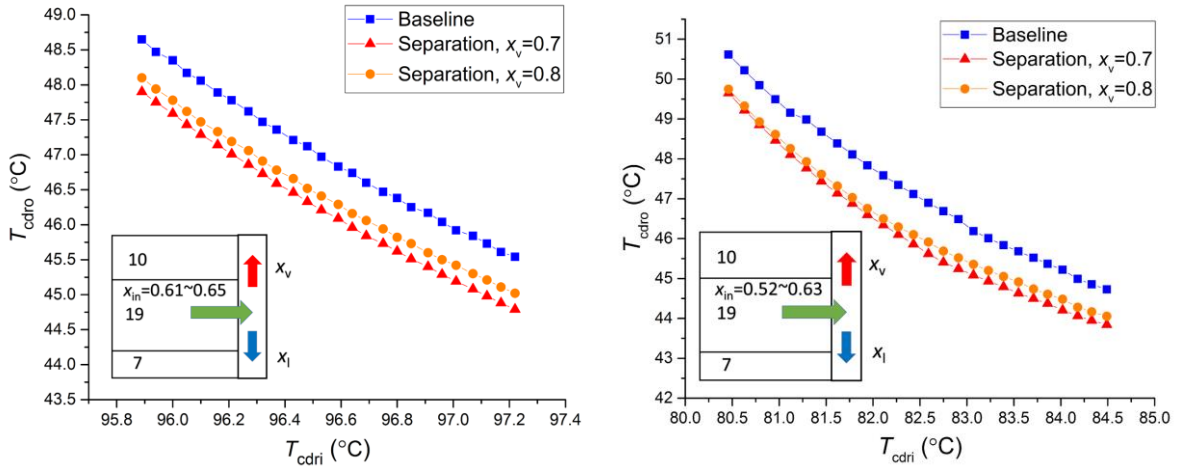

Figure 4: T_{cdro} for the two condenser at different air loads: (a) M35a, $\dot{m}_{ref}$ = 45 g/s; (b) I35a, $\dot{m}_{ref}$ = 30 g/s

The second comparison criteria is based on the fact that a better condenser can condenser more refrigerant. For the two condensers, air-side conditions are again kept the same with the first comparison. Meanwhile, refrigerant inlet conditions (T_{cdri}, P_{cdri}) are the same. The two condensers are simulated to evaluate which one can condenser more mass flow to the same outlet temperature T_{cdro}. While T_{cdri} is kept the same, various T_{cdro} represents each comparison case in Figure 6. For each simulated case of T_{cdri} and T_{cdro}, Figure 5 shows the separation condenser constantly condenses more refrigerant than the baseline, at both M35a and I35a air conditions.

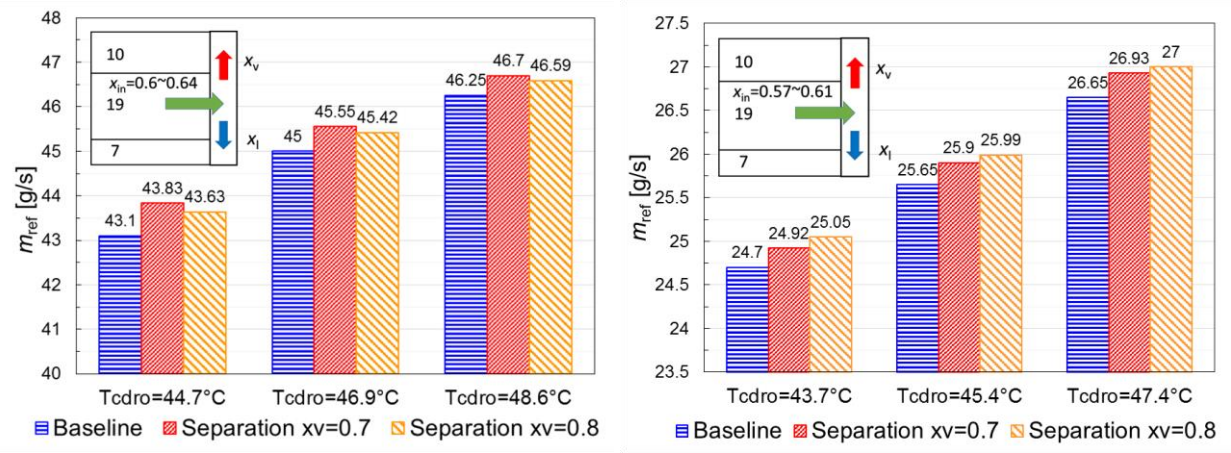

Figure 5: $\dot{m}_{ref}$ for the two condenser at different air loads: (a) M35a, T_{cdri} = 96.6°C; (b) I35a, T_{cdri} = 78.9°C

This section concludes that successful separation of liquid and vapor phase in the intermediate header of a microchannel condenser can benefit the condenser performance. A valid question would then be how much separation really exists in the intermediate header. To solve this problem, a component-level experiment facility is built up with visualization access to study the separation of two-phase flow in a vertical header as part of a MCHE.

3. EXPERIMENT SETUP

To study separation of liquid and vapor phase in vertical header of MCHE. A test section has been built as shown in Figure 6(a). The flow passes of the test section are made by 36 (21 in 1st pass, 11 in 2nd-vapor pass and 4 in 2nd-liquid pass) aluminum microchannel tubes and the header was made by circular PVC transparent tube for visualization. The tube number for each pass in the test section is the same with a real separation condenser designed for a mid-size sedan in Figure 6(b), the test of which is in progress.

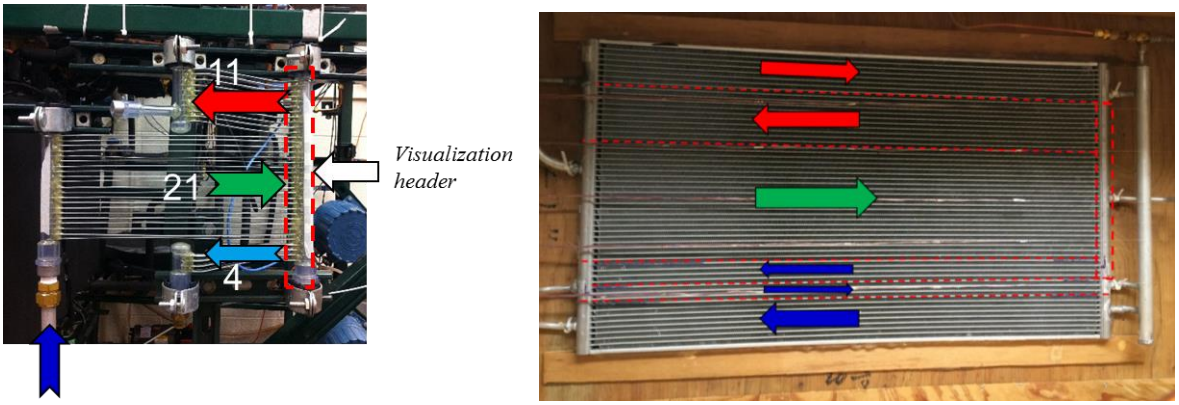

(a) (b)

Figure 6: (a) Test section (b) Location of test section in a real condenser

Inlet quality for the visualization header is controlled by 42 electric heating tapes (2 for each inlet microchannel tube). In order to simulate the case for a real condenser, sizes of the visualization header and microchannel tubes for in Figure 6(a) are selected based on the header of the real condenser in Figure 6(b). A summary of the geometry of the visualization header is found in Table 2. The header dimensions and the microchannel dimensions are chosen to be close to the real header dimensions within 10%.

Table 2: Geometries for the visualization header

Items	Values
Header length	281 mm
Header inner diameter	15.8 mm
MC tube pitch	7 mm
MC tube width	13.6 mm
MC tube thickness	1.01 mm
MC tube port number	17
MC tube port hydraulic diameter	0.65 mm

The schematic drawing of the test loop for liquid-vapor separation is shown in Figure 7. A diaphragm pump is used to supply the desired mass flow rate of the working refrigerant. Following the arrow direction, the refrigerant flow rate in subcooled state is measured in the pump discharge line by a Coriolis-type mass flow meter MF_t. Refrigerant is heated by an electric pre-heater to saturated liquid prior to the test section. Refrigerant flow is separated into two streams in the test section. When both of the 3-way valves are switched to the left, system is in the test mode. Each of two streams goes into a flash tank, named as liquid exit and vapor exit, respectively. The flash tanks collect liquid and measure the time averaged liquid mass flow rates. Meanwhile, vapor flow rate escaping from each of the flash tanks is measured by flow meters MF_v and MF_l, respectively.

Two metering valves are installed on the flow path of liquid exit and the vapor exit, respectively, with intention to simulate various downstream flow resistance of the separation header in a real condenser. Between point 1 and 2 a differential pressure transducer (ΔP) is installed to measure the pressure drop from the test section inlet to the combining point of the two flow paths and downstream pressure drop is then deduct. A high-speed CCD camera was

used to visualize the flow patterns in the test header normally at a recording speed range of 1600-2230 fps (frames per second). A further detailed description of the test section can be found in Li and Hrnjak (2015).

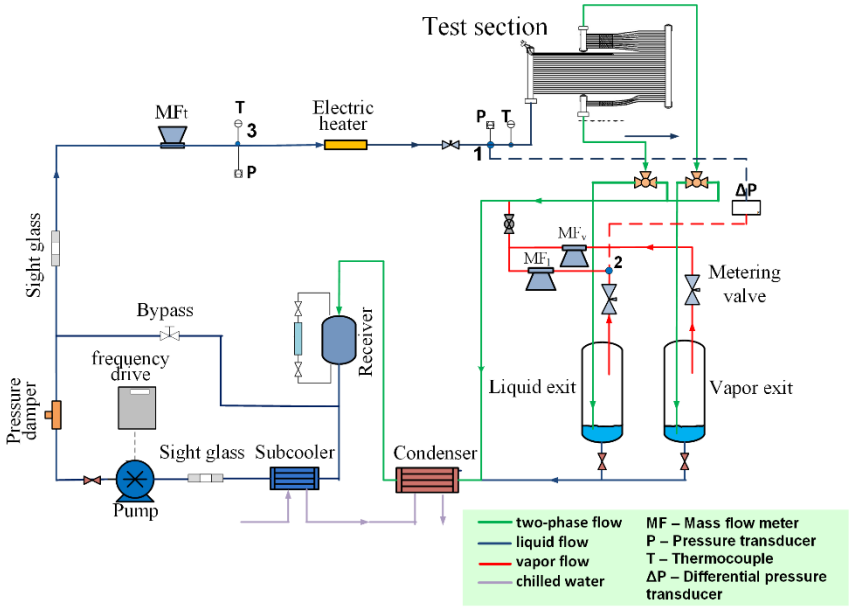

Figure 7: Experiment test loop

4. DATA REDUCTION

In order to quantify the separation performance of the header, besides two exit qualities calculated by Equation (1) and (2), two separation efficiencies are defined. Liquid separation efficiency is defined as the ratio of separated liquid which flows through the designated liquid exit of the header to the liquid supplied to the inlet. Similarly, vapor separation efficiency is evaluated as the ratio of the separated vapor which flows through the designated vapor outlet to the total amount of vapor entering the header:

$$\eta_{\mathrm{l}} = \frac{\dot{m}_{\mathrm{l,l}}}{\dot{m}_{\mathrm{l,v}} + \dot{m}_{\mathrm{l,l}}} \tag{3}$$

$$\eta_{\mathrm{v}} = \frac{\dot{m}_{\mathrm{v,v}}}{\dot{m}_{\mathrm{v,v}} + \dot{m}_{\mathrm{v,l}}} \tag{4}$$

As shown in Figure 4, the inlet refrigerant quality of the visualization header x_{in} is calculated based on the vapor and liquid mass flow rates at the two exits, as following:

$$x_{\mathrm{in}} = \frac{\dot{m}_{\mathrm{v,v}} + \dot{m}_{\mathrm{v,l}}}{\dot{m}_{\mathrm{in}}} \tag{5}$$

The overall measurement uncertainty in quality and the phase separation efficiency are calculated using the method given by Moffat (1988). If a function U is assumed to be calculated from a set of N measurements (independent variables) represented by $U = U(X_1, X_2, X_3,..., X_N)$, then the uncertainty of the result U can be determined by combining the uncertainties of the individual terms using a root-sum-square method, i.e.

$$\delta U = \sqrt{\sum_{i=1}^{N} \left(\frac{\partial U}{\partial X_i} \delta X_i \right)^2} \tag{6}$$

Using the accuracies of the measured variables presented in Table 3, the maximum measurement uncertainty for separation efficiency (η) and quality (x) are ±2.5% and ±3.7%, respectively. The zero stability for mass flow meter MF_t, is 0.0075 g/s and the zero stability for MF_v and MF_l is 0.00055 g/s.

Table 3: Measurement uncertainties

Measurement	**Unit**	**Accuracy**
Inlet liquid mass flow rate MF_t	g/s	±0.10% ± [(zero stability / flow rate) × 100]%
Vapor mass flow rate MF_v / MF_l	g/s	±0.50% ± [(zero stability / flow rate) × 100]%
Heat Input	W	± 0.2%
Liquid Level in Flash Tanks	mm	±2
Time	s	±2
Pressure	kPa	±0.5
Temperature	ºC	±0.5

5. RESULTS AND DISCUSSION

In a separation condenser, the upper vapor path and the lower liquid path would finally mix in a combining header [Figure 3(b)] or a receiver to get out of the condenser. Usually after the receiver there is a subcooling pass (Figure 2). Between the separation header exits and the mix point for vapor path and liquid path, downstream geometry and air load all affect the downstream flow resistance and give different pressure drop, which set the boundary conditions for pressure at liquid and vapor exits and alter the flow separation in the header.

In experiments, this effect can be simulated by adjusting the two metering valves downstream the two flash tanks as shown in Figure 7. In initial experiments, the two metering vales are left with the maximum opening, which will give the test header minimum downstream flow resistance.

R134a is tested with pressure at 500±20 kPa. Total mass flow rate is varied from 8.4 g/s to 30 g/s, which corresponds to mass flux of 54 kg/m^2·s-193 kg/m^2·s through the microchannel tubes in the first pass of the condenser. Inlet quality to the header is controlled over a range of 0.05 to 0.25, which is on the lower end of the quality in a real condenser. However, it is where separation phenomenon and mechanism change, therefore, this range is of interest to study phase separation as a starter.

Figure 8 and Figure 9 present the results of η_l, η_v, x_l, and x_v for 4 typical mass flow rates: 10 g/s, 16 g/s, 20 g/s, and 25 g/s. At low mass flow rates, inlet quality shows strong impact on liquid separation. As shown in Figure 8(a), at 10 g/s with x=0.06, η_l is 0.38, which means more than of the liquid is sending out from the vapor exit. However, as x increases to 0.14, η_l increases dramatically to 1, at this time no liquid is escaping from the vapor exit. Similar with η_l, x_v is high at low mass flow rate (10 g/s) and high inlet quality ($x_{in} > 0.15$). But at higher mass flow rate, due to the large initial upward velocity of liquid after impinging on the wall, both η_l and x_v drop dramatically, as shown in Figure 8(a) and 9(b). It is evident that η_l has the same trend with x_v because high η_l means little liquid going up, which gives a high x_v. It is possible that x_v would become smaller and have less dependence on x_{in} at an even higher mass flow rate beyond the current range of test conditions.

For η_v in Figure 8(b), except for 10 g/s under 0.15 inlet quality, η_v keeps dropping with the increase of inlet quality. The dropping amount varies from 20% to 14% as mass flow rate increases. It is apparent that both high mass flow rate and high inlet quality are detrimental to the separation of vapor. It is extrapolated that with higher amount of vapor entering the header, more vapor would highly mix the flow inside the header and make the flow approach to homogeneity, thus, more vapor is getting out through the liquid exit.

As shown in Figure 9, x_l could always be maintained at a lower value than its corresponding inlet quality while x_v higher than the inlet quality. This means separation exists in the header, but not perfect as it is influenced by x_{in} and $\dot{m}_{in}$. The smallest difference between x_{in} and x_l is 29% at 25 g/s and inlet quality of 0.21.

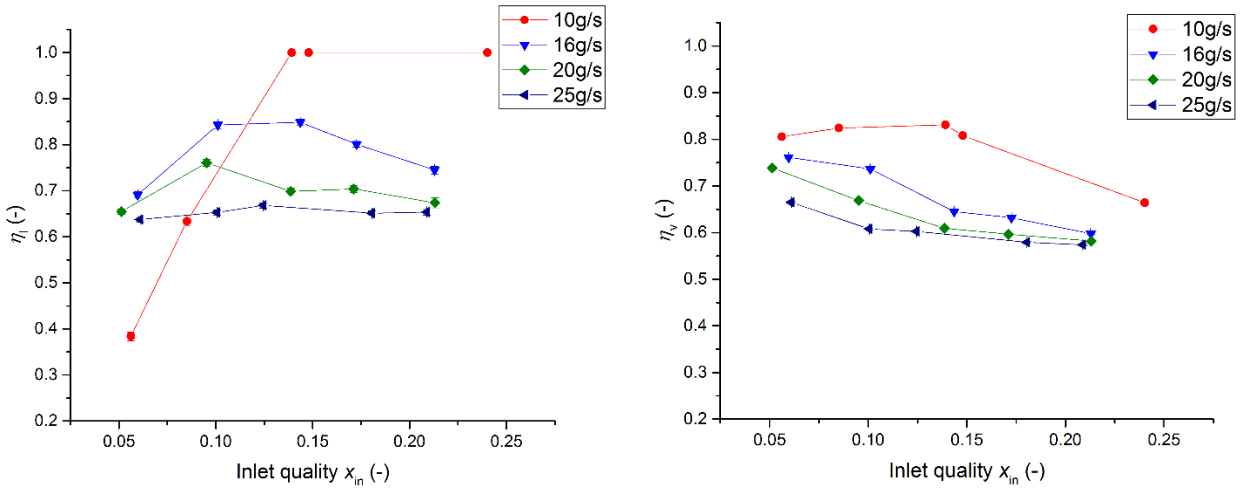

Figure 8: (a) Liquid separation efficiency vs. inlet quality; (b) Vapor separation efficiency vs. inlet quality

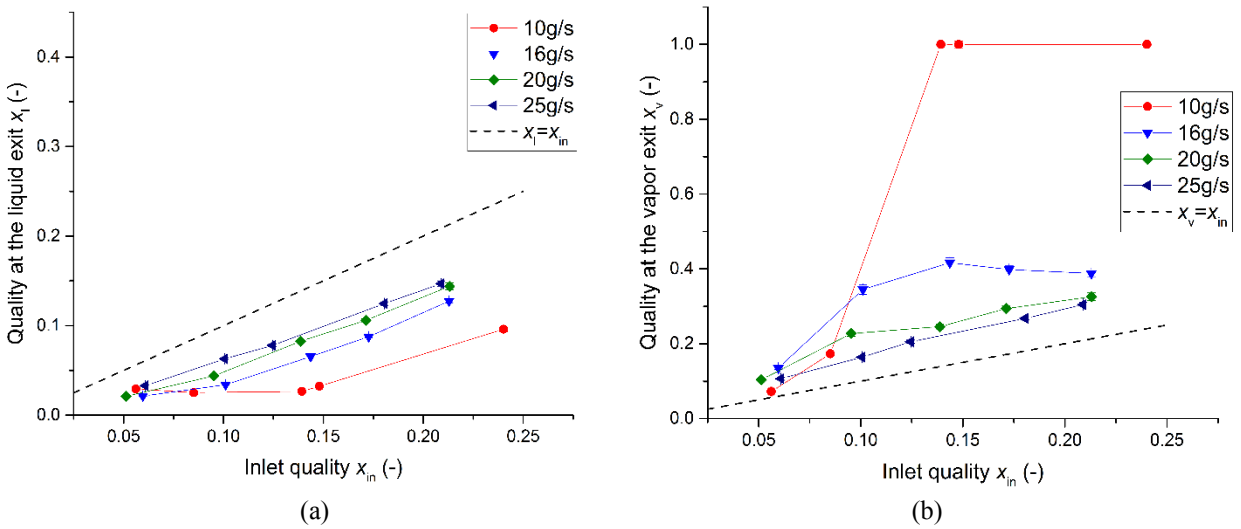

Figure 9: (a) Liquid exit quality vs. Inlet quality; (b) Vapor exit quality vs. Inlet quality

Figure 10 presents different separation phenomenon at low mass flow rate and high mass flow rate. At low mass flow rates of 10 g/s, inlet quality shows strong impact on separation. η_l changes from 0.38 to 1 while η_v drops from 0.83 to 0.66. At low qualities and low mass flow rates, for example 10 g/s at x=0.05 in Figure 9(a), the header is almost filled with liquid. It is a consequence of difficulty to send liquid through the liquid exit out. In these operating conditions pressure in the second header is low. Liquid flow through the second liquid pass is provided mostly by hydrostatic head (ρgh), so that liquid is being accumulated in the header to increase flow rate. Consequently liquid separation is poor and much liquid leaves through the vapor exit resulting in a η_l as low as 0.38.

When the quality is increased to x=0.15 at the same flow rate of 10 g/s, η_l increases dramatically to 1 and x_v=1. Pressure in the second header had increased and mass flow rate of liquid is reduced resulting in good drainage of the liquid providing possibility for a good separation in the second header. Liquid coming from microchannels falls relatively unobstructed to the bottom of the header while vapor goes up passing falling liquid easy thanks to low vapor flow and thus velocity. With further increase of inlet quality to 0.25, η_l is still 1 while η_v drops to 0.664. Visualization shows that vapor extends to the liquid exit. x_l is 0.096.

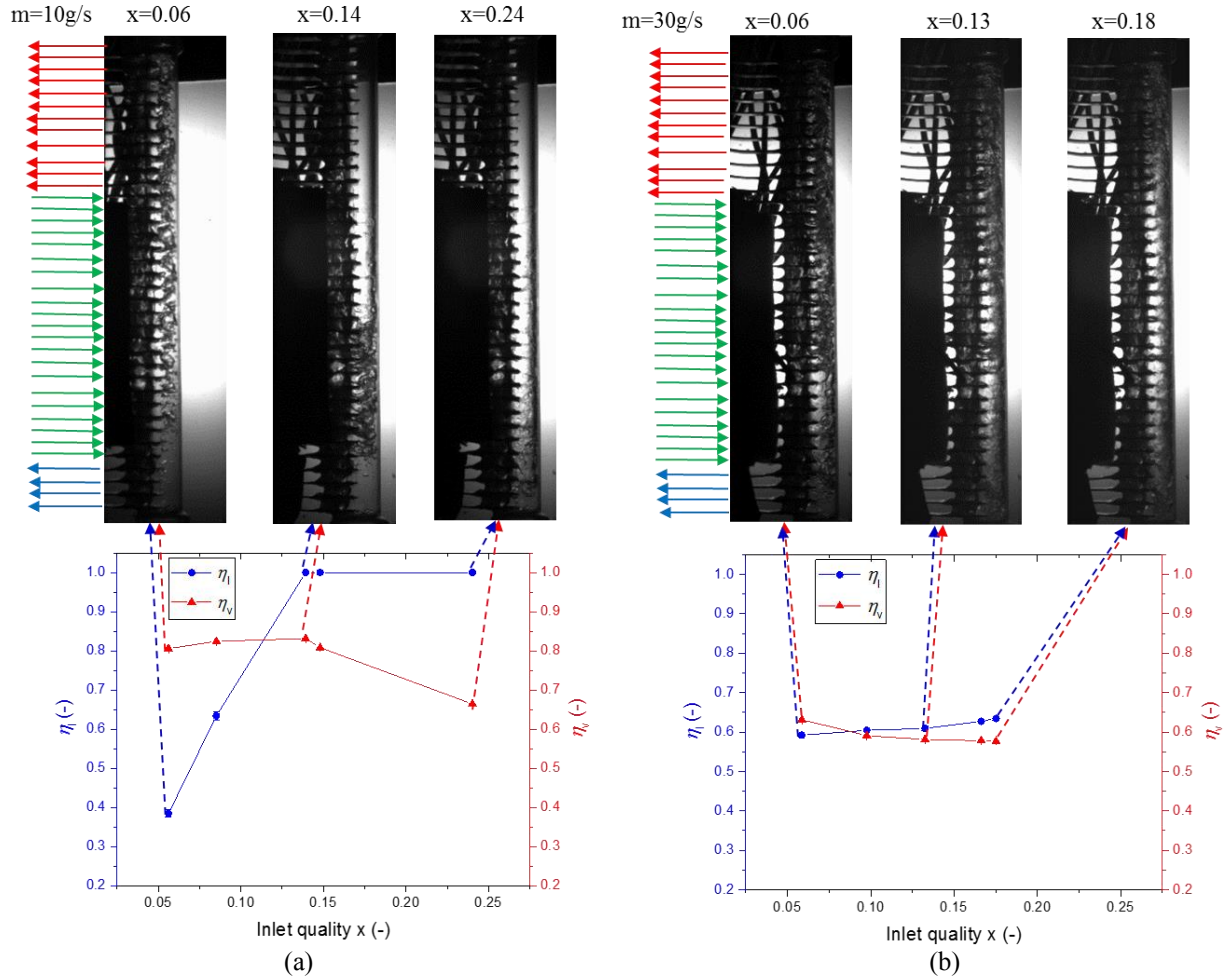

Figure 10: Separation phenomenon at (a) 10 g/s; (b) 30g/s

At high mass flow rate 30 g/s, Figure 10(b) shows: 1) both liquid and vapor separation efficiencies drop compared with the same quality at 10 g/s; 2) liquid or vapor separation efficiency does not change with changing inlet quality as dramatically as it does at low mass flow rate. Two-phase flow coming out of the inlet microchannel tubes first splashes on the inner wall of the header, then is divided almost equally into upward and downward streams. For the three cases of x_{in} (0.06, 0.13, and 0.18), x_v (0.09, 0.19, and 0.25) is close to respective inlet quality.

6. CONCLUSION

The separation phenomena of liquid-vapor two-phase flow in a vertical header of a separation condenser is analyzed by both quantitative and visual methods. Separation is proved by the model to be beneficial to heat exchange and to be influenced by separation results in the header. T_{cdro} of the separation condenser is lower than the baseline by up to 1.1°C. Experimental validation in the MAC system is underway.

Visualization is taken in the vertical header (D=15.8 mm) of a mid-size automobile MC condenser. For the inlet quality on the lower end of that in a real condenser, separation is good at mass flow rate of 10 g/s / mass flux of 70 kg/(m^{2}s) but turns small when mass flow rate is over 20 g/s. Inlet quality loses its impact on separation at mass flow rate over 20 g/s. Separation is better when downward liquid and upward vapor flows can pass each other. As mass flow increases velocities increase, especially when combined with increasing quality. These two effects both mix phases and make separation efficiencies drop.

Nomenclature

D	diameter	(mm)	**Subscripts**	
$\dot{m}$	mass flow rate	(g/s)	cdri	condenser refrigerant inlet
MAC	mobile air conditioning		cdro	condenser refrigerant outlet
MC	microchannel		in	inlet
MCHE	microchannel heat exchanger		l (1st)	liquid phase
P	pressure	(kPa)	l (2nd)	liquid path
T	temperature	(°C)	ref	refrigerant
x	vapor quality		v (1st)	vapor phase
Greeks			v (2nd)	vapor path
η_l	liquid separation efficiency	(-)		
η_v	vapor separation efficiency	(-)		

REFERENCES

Chang, Y.J., Wang, C.C., 1997, A Generalized Heat Transfer Correlation for Louver Fin Geometry, *Int. J. Heat Mass Transfer*, vol. 40 no.3: p. 533-544.

Chang, Y.J., Wang, C.C., 1996, Air Side Performance of Brazed Aluminum Heat Exchangers, *J. Enhanced Heat Transfer*, vol. 3 no.1: p. 15-28.

Churchill S.W., 1977, Friction-factor equation spans all fluid-flow regimes, *Chem. Eng.*, vol. 84 no.24: p. 91-92.

Cavallini, A., Doretti, L., Matkovic, M., Rossetto, L., 2006, Update on Condensation Heat Transfer and Pressure Drop inside Minichannels, *Heat Transfer Engineering*, vol 27 no.4: p. 74-87.

Cavallini, A., Del Col, D., Matkovic, M., and Rossetto, L., 2009, Frictional Pressure Drop During Vapour–Liquid Flow in Minichannels: Modelling and Experimental Evaluation, *Int. J. Heat and Fluid Flow*, vol. 30 no.1: p. 131-139.

Gnielinski, V., "New Equation of Heat and Mass Transfer in Turbulent Pipe and Channel Flow," Int. Chem. Eng., 16(2):359-368, 1976.

Li, H., Hrnjak, P., 2014, Quantification of Liquid Refrigerant Distribution in Parallel Flow Microchannel Heat Exchanger Using Infrared Thermography, *International Refrigeration and Air Conditioning Conference*, Paper 1374.

Li, J., Hrnjak, P., 2015, Phase Separation in Second Header of MAC Condenser, *SAE Technical Paper* 2015-01-1694.

Moffat, R.J., 1988, Describing the Uncertainties in Experimental Results, *Exp. Therm. Fluid Sci.*, vol. 1 no. 1: p. 3-17.

Oh, K., Lee, S., Park, T., Kim, Y., 2003, Multistage Gas and Liquid Phase Separation Condenser," *U.S. Patent* US2003/0217567.

SAE International, 2008, Procedure for Measuring System COP [Coefficient of Performance] of a Mobile Air Conditioning System on a Test Bench, SAE Surface Vehicle Standard J2765 OCT2008, Atlanta GA.

Tuo, H., Hrnjak, P., 2013, Effect of the header pressure drop induced flow maldistribution on the microchannel evaporator performance, *Int. J. of Refrig.*, vol. 36, no. 8: p. 2176-2186.

Wu, D., Wang, Z., Lu, G., Peng, X., 2010, High-Performance Air Cooling Condenser With Liquid–Vapor Separation, *Heat Trans. Eng.*, vol. 31, no. 12: p. 973-980.

Xu, J., Hrnjak, P., 2016, Refrigerant-Oil Flow at the Compressor Discharge, *SAE Technical Paper* 2016-01-0247.

Ye, L., Tong, M.W., Zeng X., 2009, Design and Analysis of Multiple Parallel-Pass Condensers, *Int. J. Refrig.*, vol. 32, no. 6: p. 1153-1161.

Zhong, T.M., Chen, Y., Hua, N., Zheng, W.X., Luo, X.L., Mo. S.P., 2014, In-tube Performance Evaluation of an Air-cooled Condenser With Liquid–Vapor Separator, *Applied Energy*, vol. 136: p. 968-978.

Zou, Y., Hrnjak, P., 2013, Refrigerant Distribution in the Vertical Header of the Microchannel Heat Exchanger - Measurement and Visualization of R410A Flow, *Int. J. of Refrig.*, vol. 36 no. 8: p. 2196-2208.

ACKNOWLEDGEMENT

The authors thankfully acknowledge the support provided by the Air Conditioning and Refrigeration Center at the University of Illinois at Urbana-Champaign.